Carbohydrate Research 344 (2009) 642–647

Contents lists available at ScienceDirect

Carbohydrate Research

journal homepage: www.elsevier.com/locate/carres

Characterization of the interaction between 2′-deoxyuridine and human serum albumin

Fengling Cui [a,*], Yinghua Yan [a], Qiangzhai Zhang [a], Juan Du [b], Xiaojun Yao [b,*], Guirong Qu [a], Yan Lu [a]

[a] School of Chemistry and Environmental Science, Key Laboratory for Yellow River and Huai he River Water Environment and Pollution Control Ministry of Education, Henan Normal University, Xinxiang 453007, PR China
[b] Department of Chemistry, Lanzhou University, Lanzhou 730000, PR China

ARTICLE INFO

Article history:
Received 22 September 2008
Received in revised form 11 January 2009
Accepted 13 January 2009
Available online 19 January 2009

Keywords:
2′-Deoxyuridine
Human serum albumin (HSA)
Fluorescence spectroscopy
Synchronous fluorescence spectrum
Molecular modeling

ABSTRACT

The binding of 2′-deoxyuridine to human serum albumin (HSA) was investigated by fluorescence spectroscopy in combination with molecular modeling under simulation of physiological conditions. The quenching mechanism was suggested to be static according to the fluorescence measurement. The thermodynamic parameters: enthalpy change (ΔH) and entropy change (ΔS) were calculated to be −18.87 kJ/mol and 24.00 J/(mol K) according to the Vant'Hoff equation. These data suggest that hydrophobic interactions are the predominant intermolecular forces stabilizing the complex. Experimental results are in agreement with the results obtained by molecular modeling study. In addition, the effects of common ions on the binding constants were also studied at room temperature.

1. Introduction

Nucleosides and their derivatives exhibit significant antitumor, antiviral, and antibacterial activities.[1–3] 2′-Deoxyuridine (Structure 1) is an important synthon, which is widely used to manufacture anticancer, antimicrobial, and antiviral medicines. Therefore, it is of importance to investigate the interaction between 2′-deoxyuridine and human serum albumin (HSA).

HSA is the most abundant protein constituent of blood plasma and serves as a protein storage component. The three-dimensional structure of human serum albumin has been determined through X-ray crystallographic measurement. This globular protein, which consists of a single polypeptide chain of 585 amino acid residues, has important physiological functions. It considerably contributes to colloid osmotic blood pressure and is involved in the transport and distribution of many molecules and metabolites, such as fatty acids, amino acids, hormones, cations and anions, and many diverse drugs.[4] HSA can bind and carry through the bloodstream poorly water-soluble drugs, including anticoagulants, tranquilizers, and anesthetics.[5,6] It has been shown that the distribution, free concentration, and the metabolism of various drugs can be significantly altered as a result of their binding to HSA.[7] Drug interactions with proteins will in most cases significantly affect the elimination rate of the drug. Up to now, extensive investigations on interactions between proteins and components of living systems or pharmaceutical molecules have been carried out,[8,9] because such studies can provide information on the features that affect the therapeutic effect of drugs.

In this paper, we studied the interaction of 2′-deoxyuridine with HSA at three temperatures under simulation of physiological conditions utilizing fluorescence in combination with molecular modeling. In the meantime, the binding mechanism of 2′-deoxyuridine to HSA was discussed, and the binding parameters of the reaction were calculated according to fluorescence data. In addition, the effects of other ions on binding constants were also investigated.

2. Results and discussion

2.1. Binding mechanism and binding constants

2.1.1. Fluorescence quenching spectral studies

The fluorescence of HSA originates from the tryptophan, tyrosine, and phenylalanine residues.[10] Actually, the intrinsic fluorescence of HSA is essentially due to tryptophan alone, because phenylalanine has a very low quantum yield and the fluorescence of tyrosine is almost totally quenched if it is ionized or is near an amino group, a carboxyl group, or a tryptophan residue.[11] When small molecules bind to HSA, changes of intrinsic fluorescence intensity of HSA are induced by the microenvironment of tryptophan residues. The fluorescence emission spectra of HSA at various concentrations of 2′-deoxyuridine are shown in Figure 1. Obviously, HSA has a strong fluorescence emission band at 350 nm at

* Corresponding authors. Tel.: +86 373 3326335; fax: +86 373 3326336 (F.C.).
E-mail addresses: cuifl718@hotmail.com (F. Cui), xiaojunyao@yahoo.com (X. Yao).

0008-6215/$ - see front matter © 2009 Elsevier Ltd. All rights reserved.
doi:10.1016/j.carres.2009.01.009

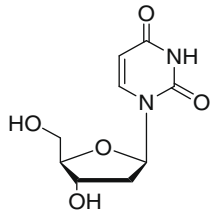

Structure 1. The molecular model of 2′-deoxyuridine ($C_9H_{12}N_2O_5$, molecular weight: 228.2).

an excitation wavelength of 282 nm, which is mainly due to its single tryptophan residue, while 2′-deoxyuridine had no intrinsic fluorescence under the present experimental conditions. The fluorescence emission intensity of HSA decreases regularly from 85.9931 to 64.8536 while increasing the concentration of 2′-deoxyuridine from 0 to 5.0×10^{-5} mol L^{-1}. The strong quenching of HSA fluorescence clearly indicates that the interaction between 2′-deoxyuridine and HSA takes place and results from microenvironment changes of the tryptophan residues and the tertiary structure of HSA.[12]

Synchronous fluorescence spectra are frequently used to characterize the interaction between molecular probes and proteins since it can provide information on the molecular microenvironment in the vicinity of the chromosphere molecules. According to Miller,[13] with large $\Delta\lambda$ values such as 60 nm, the synchronous fluorescence of HSA is characteristic of tryptophan residues. When the $\Delta\lambda$ value is 15 nm, the synchronous fluorescence is characteristic of tyrosine residues.[14] Synchronous fluorescence spectra of HSA upon addition of various concentrations of 2′-deoxyuridine for $\Delta\lambda$ = 15 (a) and 60 nm (b) are shown in Figure 2. Addition of the drug leads to a dramatic decrease in the synchronous fluorescence intensity with distinct shift of spectral peak from 298 to 301 nm (Fig. 2a) and from 339 to 344 nm (Fig. 2b), respectively. It is considered that the maximum emission wavelength (λ_{max}) of the tryptophan residues is related to the polarity of the microenvironment. Absorption at 330–332 nm suggests that tryptophan residues are located in the non-polar region, that is, they are buried in a hydrophobic cavity of HSA; absorption at 350–352 nm indicates that tryptophan residues are exposed to water, that is, the hydrophobic cavity in HSA is disaggregated and the structure of HSA is looser. Thus, Figure 2b shows distinctly that 2′-deoxyuridine mainly binds to the hydrophobic cavity of HSA, which is in agreement with the results from molecular modeling and the thermodynamic parameters obtained from the experimental data. It was also indicated that the polarity around the tryptophan residues was increased and the hydrophobicity was decreased. In Figure 2a, the fluorescence of tyrosine residues was also quenched by 2′-deoxyuridine with a slight shift of emission to a longer wavelength from 298 to 301 nm. It is suggested that the polarity around the tyrosine residues also increased. The increase in fluorescence intensity for tyrosine residues was more definite than for tryptophan residues, which may indicate that the distance between 2′-deoxyuridine and tryptophan residues is larger.

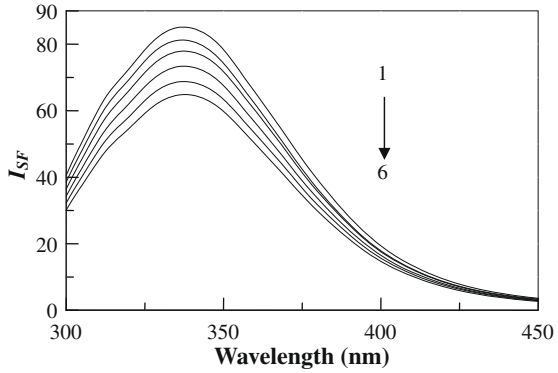

Figure 1. The fluorescence emission spectra of 2′-deoxyuridine various concentrations and an excitation wavelength of 282 nm in Tris–HCl buffer solution (pH 7.4) at 27 °C: $C_{HSA} = 0.8\times10^{-6}$ M, while the 2′-deoxyuridine corresponding to 0, 0.2, 0.4, 0.6, 0.8, and 1.0×10^{-5} M is denoted by numerals 1–6.

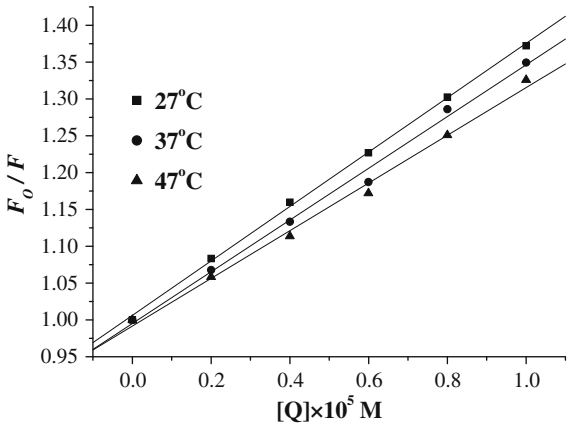

Figure 3. Stern–Volmer curves of 2′-deoxyuridine quenching the fluorescence of HSA at pH 7.40: C_{HSA} and $C_{2'\text{-deoxyuridine}}$ are the same as those in Figure 1.

2.1.2. Quenching mechanisms study

The static quenching and dynamic quenching were differentiated by monitoring at different temperatures. The quenching rate

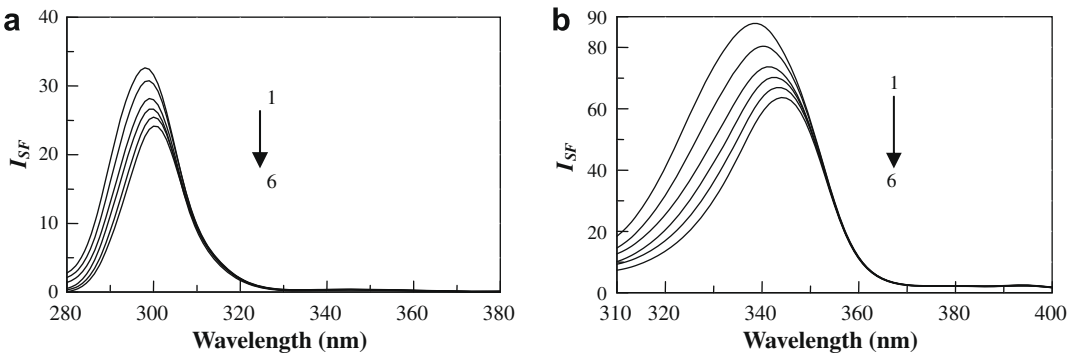

Figure 2. Synchronous fluorescence spectra of 2′-deoxyuridine various concentrations while the $\Delta\lambda$ = 15 nm (a) and $\Delta\lambda$ = 60 nm (b): C_{HSA} and $C_{2'\text{-deoxyuridine}}$ are all the same as those in Figure 1.

constants decrease with increasing temperature for static quenching, but a reverse effect is observed for dynamic quenching.[15] The possible quenching mechanism can be investigated by the fluorescence quenching spectra of HSA. The F_0/F-[Q] (Stern–Volmer) curves of 2′-deoxyuridine with HSA at different temperatures (27, 37, and 47 °C) are shown in Figure 3.

It can be seen from Figure 3 that the Stern–Volmer plots are linear and the slopes decrease with increasing temperature. This indicates that the interaction between 2′-deoxyuridine and HSA is a static quenching. In order to confirm this point, the procedure was assumed to be dynamic quenching. The fluorescence quenching data were analyzed by the Stern–Volmer equation 1,

$$F_0/F = 1 + K_q\tau_0[Q] = 1 + K_{sv}[Q], \quad (1)$$

where F and F_0 are the fluorescence intensities with and without quenchers. K_q, K_{sv}, τ_0, and [Q] are, respectively, the quenching rate constants of the molecule, the Stern–Volmer quenching constant, and the average lifetime of the molecule without quencher and increasing concentration of quencher. Obviously,

$$K_{sv} = K_q\tau_0. \quad (2)$$

Because the fluorescence lifetime of HSA is 10^{-8} s,[16] an approximate quenching constant (K_q, L mol^{-1} s^{-1}) could be obtained according to Eq. 2. The results are listed in Table 1 together with correlation coefficients.

The maximum scattered collision quenching constant K_q of various quenchers with HSA is 2.0×10^{10} L mol^{-1} s^{-1}.[17] Obviously, the rate constant of the protein quenching process initiated by 2′-deoxyuridine is greater than that of the scattered procedure. This shows that the quenching is not initiated by dynamic collision but results from formation of a complex.

In drug-protein binding studies, several equations have been used for binding constant calculation. One frequently used is the Scatchard equation[18]:

$$r/D_f = nK - rK, \quad (3)$$

Table 1
Quenching constant (L mol^{-1} S^{-1}) between 2′-deoxyuridine and HSA by Stern–Volmer equation

T (°C)	Stern–Volmer equation	K_q (L mol^{-1} S^{-1})	R
27	$Y = 0.9966 + 0.3550 \times 10^5[Q]$	3.550×10^{12}	0.9997
37	$Y = 0.9952 + 0.3510 \times 10^5[Q]$	3.510×10^{12}	0.9972
47	$Y = 0.9916 + 0.3236 \times 10^5[Q]$	3.236×10^{12}	0.9971

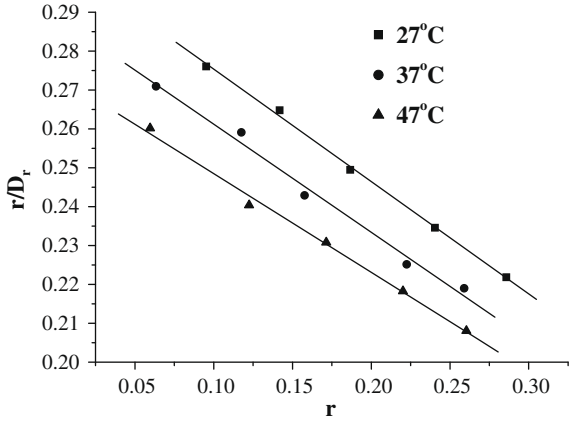

Figure 4. Scatchard curves for 2′-deoxyuridine quenching the fluorescence of HSA: the $C_{2'\text{-deoxyuridine}}$ and C_{HSA} are the same as those in Figure 1.

Table 2
Binding constants (L mol^{-1}) between 2′-deoxyuridine and HSA by Lineweaver–Burk equation

T (°C)	Lineweaver–Burk equation	K (L mol^{-1})	R
27	$Y = 1.277 \times 10^{-2} + 0.3691 \times 10^{-6}[Q]$	3.460×10^4	0.9988
37	$Y = 0.847 \times 10^{-2} + 0.3127 \times 10^{-6}[Q]$	2.709×10^4	0.9992
47	$Y = 0.584 \times 10^{-2} + 0.3434 \times 10^{-6}[Q]$	1.701×10^4	0.9992

where r is the number of drug molecules bound per mol of protein, D_f is the concentration of unbound drug, K is the binding constant, and n is the number of binding sites. The Scatchard plots for the 2′-deoxyuridine/HSA system at different temperatures are shown in Figure 4. The linearity of the Scatchard plot indicates that 2′-deoxyuridine binds to a single class of binding sites on HSA, which is in full agreement with the number of binding sites n. The binding constants (K, Table 2) agree very closely with those obtained by the modified Stern–Volmer equation. In addition, there is a strong interaction between 2′-deoxyuridine and HSA. The binding constant decreases while the temperature increases, resulting in a decrease in the stability of the 2′-deoxyuridine/HSA complex, but the effect of temperature is very small. Thus, the quenching efficiency of 2′-deoxyuridine to HSA is obviously not diminished when the difference in temperature is not large.

Because the binding site is approximately 1, the binding constants obtained by using the Lineweaver–Burk equation are applied in the discussion of binding modes. The static quenching equation is

$$(F_0 - F)^{-1} = F_0^{-1} + K^{-1}F_0^{-1}[Q]^{-1}, \quad (4)$$

where K is the binding constant of the drug with HSA, which can be calculated from the slope and intercept of the Lineweaver–Burk curves as shown in Figure 5 (K = intercept/slope). The results are listed in Table 2.

This result confirm that the binding between 2′-deoxyuridine and HSA is important and the effect of temperature is small. Thus, 2′-deoxyuridine can be stored and removed by the protein in vivo.

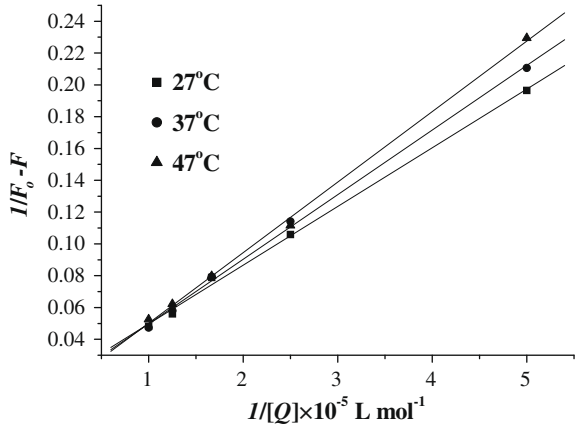

Figure 5. Lineweaver–Burk curves for 2′-deoxyuridine quenching the fluorescence of HSA at pH 7.40: C_{HSA} and $C_{2'\text{-deoxyuridine}}$ are the same as those in Figure 1.

Table 3
Thermodynamic parameters of 2′-deoxyuridine–HSA interaction at pH 7.4

Complex	T (°C)	ΔG (kJ mol^{-1})	ΔH (kJ mol^{-1})	ΔS (J mol^{-1} K)
2′-Deoxyuridine–HSA	27	−26.07	−18.87	24.00
	37	−26.31		
	47	−25.92		

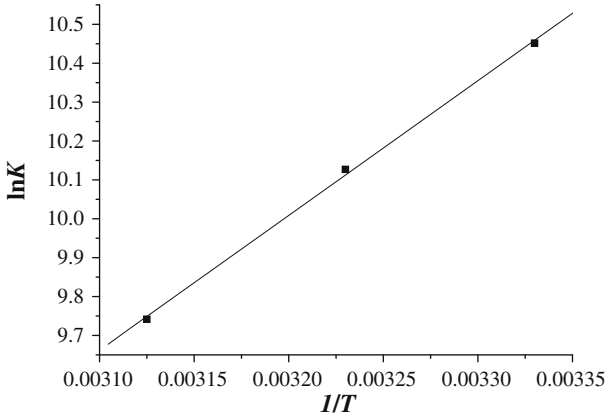

Figure 6. Van't Hoff plot for the interaction of 2′-deoxyuridine and HSA.

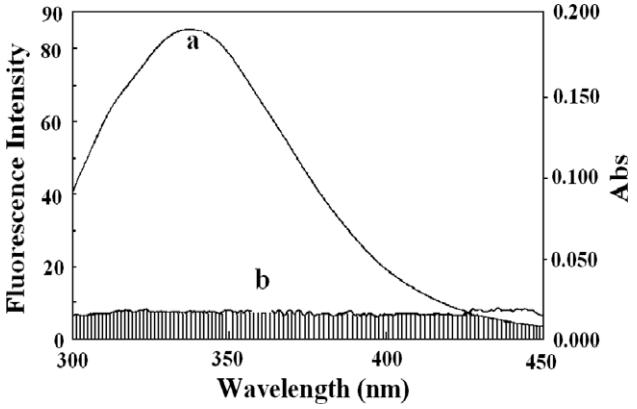

Figure 7. Overlap of UV absorption spectra of 2′-deoxyuridine and the fluorescence emission spectra of HSA. (a) The fluorescence emission spectrum of HSA (0.8×10^{-6} M); (b) the UV absorption spectrum of 2′-deoxyuridine (0.2×10^{-5} M).

2.2. Binding modes

The acting forces between a drug and a biomolecule involves weak interactions such as hydrogen bond formation, van der Waals forces, electrostatic forces, and hydrophobic interaction.[19] Thermodynamic parameters such as enthalpy change (ΔH) and entropy change (ΔS) of the binding reaction are the main evidence for confirming binding modes. From the thermodynamic standpoint, $\Delta H > 0$ and $\Delta S > 0$ implies a hydrophobic interaction; $\Delta H < 0$ and $\Delta S < 0$ reflects the van der Waals force or hydrogen bond formation; and $\Delta H \approx 0$ and $\Delta S > 0$ suggests an electrostatic force.[20]

The temperature-dependence of the binding constants was studied at three different temperatures (27, 37, and 47 °C) considering that HSA could not undergo any structural degradation. Because the temperature effect was very small, the interaction enthalpy change could be regarded as a constant if the temperature range is not too large. The thermodynamic parameters (Table 3) were determined from the linear Van't Hoff plot (Fig. 6) according to the thermodynamic Eqs. 5 and 6, where R is the gas constant, by plotting the binding constants (K value in Table 2) according to the Van't Hoff equation

$$\ln K = -\Delta H/RT + \Delta S/R \quad (5)$$

$$\Delta G = \Delta H - T\Delta S = -RT \ln K \quad (6)$$

As shown in Table 3, ΔG and ΔH were found negative, and ΔS was positive. Therefore, the formation of the 2′-deoxyuridine–HSA coordination compound was spontaneous and the exothermic reaction accompanied a positive ΔS value. According to the concepts of Neméthy and Scheraga,[21] Timasheff,[22] and Ross and Subramananian,[20] the positive ΔS value is frequently taken as evidence for hydrophobic interaction. Furthermore, specific electrostatic interactions between ionic species in aqueous solution are characterized by a positive value of ΔS and a negative ΔH value. Accordingly, it was not possible to account for the thermodynamic parameters of the 2′-deoxyuridine–HSA complex on the basis of a single interaction. It was more likely that both hydrophobic and electrostatic interactions are involved in the binding process. But 2′-deoxyuridine must be considered to be largely unionized under the experimental conditions, as could be expected from its structure. Thus, electrostatic interaction could not play a major role in the binding, and binding of 2′-deoxyuridine to HSA is then mainly based on hydrophobic interactions.

Table 4
The binding constants (K, L mol^{-1}) between 2′-deoxyuridine and HSA at 27 °C in the presence of common ions

Ions	$K(10^4)$	R_{HSA}	Ions	$K(10^4)$	R_{HSA}
K^+	2.913	0.9996	Zn^{2+}	1.757	0.9997
Ca^{2+}	1.068	0.9996	Pb^{2+}	2.244	0.9997
NH_4^+	2.042	0.9974	Mg^{2+}	0.536	0.9974
Bi^{3+}	2.899	0.9999	F^-	3.220	0.9982
Cu^{2+}	2.951	0.9981	SiO_3^{2-}	0.180	0.9998
$C_2O_4^{2-}$	1.057	0.9998	NO_3^-	3.198	0.9990
Mn^{2+}	2.206	0.9999	CO_3^-	0.559	0.9984
Cd^{2+}	1.062	0.9996	Al^{3+}	3.133	0.9991
Hg^{2+}	0.277	0.9994	Co^{2+}	2.072	0.9998

2.3. Binding distance

According to the Föster's non-radiative energy transfer theory,[23] the rate of energy transfer depends on: (i) the relative orientation of the donor and acceptor dipoles, (ii) the extent of overlap of the emission spectrum of the donor with the absorption spectrum of the acceptor, and (iii) the distance between the donor and the acceptor. The energy transfer effect is related not only to the distance between the acceptor and the donor, but also to the critical energy transfer distance R_0, that is,

$$E = R_0^6/(R_0^6 + r^6), \quad (7)$$

where r is the distance between the acceptor and the donor and R_0 is the critical distance when the transfer efficiency is 50%, which can be calculated by

$$R_0^6 = 8.8 \times 10^{-25} k^2 N^{-4} \phi J, \quad (8)$$

where k^2 is the spatial orientation factor between the emission dipole of the donor and the absorption dipole of the acceptor. The dipole orientation factor k^2 is the least certain parameter in calculation of the critical transfer distance, R_0. Although theoretically k^2 can range from 0 to 4, the extreme values require very rigid orientations. If both the donor and acceptor are tumbling rapidly and free to assume any orientation, then k^2 equals 2/3.[24] If only the donor is free to rotate, then k^2 can vary from 1/3 to 4/3.[25,26] N is the refractive index of the medium, ϕ is the fluorescence quantum yield of the donor, and J is the overlap integral of the fluorescence emission spectrum of the donor, and the absorption spectrum of the acceptor, given by

$$J = \sum F(\lambda)\epsilon(\lambda)\lambda^4 \Delta\lambda \Big/ \sum F(\lambda)\Delta\lambda, \quad (9)$$

where $F(\lambda)$ is the fluorescence intensity of the fluorescent donor in wavelength (λ) and is dimensionless, $\varepsilon(\lambda)$ is the molar absorption coefficient of the acceptor in wavelength. The energy transfer efficiency is frequently calculated from the relative fluorescence yield in the presence (F) and absence (F_0) of acceptor

$$E = 1 - F/F_0 \quad (10)$$

J could be evaluated by integrating the spectra in Figure 8. It was reported for HSA that $k^2 = 2/3$, $\phi = 0.118$, and $N = 1.336$.[27] The value of the overlapped integral calculated from Figure 7 was 3.0933×10^{-14} cm^3 L mol^{-1}. Based on these data, it results that r the distance between 2′-deoxyuridine and the tryptophan residue in HSA is 4.75 nm, a value smaller than 7 nm, confirming the static quenching interaction between 2′-deoxyuridine and HSA.

2.4. The effects of other ions on the binding constants

The HSA molecule contains elements such as S, P, Cu, and Mn among others. In addition, some trace metal ions occur in vivo, which have definite ability to bind proteins.[28,29] To investigate the effect of coexisting ions, the binding constants in the presence of other ions were investigated at 27 °C under the experimental conditions. The results listed in Table 4 show that the binding constants between 2′-deoxyuridine and HSA decrease in the presence of other ions, implying some binding between metal ions and HAS. This confirms that the presence of other ions directly affects the binding between 2′-deoxyuridine and HSA. The competition between coexistent ions and 2′-deoxyuridine decreases the binding constant between 2′-deoxyuridine and HSA, which causes the shortening of the storage time of the nucleotide drug in the blood plasma and enhances the maximum effectiveness of the nucleotide drug.

2.5. Molecular modeling study

Molecular modeling was further employed to improve our understanding of the interaction of 2′-deoxyuridine and HSA. From the 3-D structure of crystalline albumin, it is known that HSA comprises three homologous domains (denoted I, II, and III): I comprises residues 1–195; II residues 196–383; and III, residues 384–585, each with two subdomains, A and B possessing common structural motifs. It is suggested that the principal regions of ligand binding to HSA are located in hydrophobic cavities in subdomains IIA and IIIA, which are consistent with site I and site II, respectively, and one tryptophan residue (Trp-214) of HSA is in subdomain IIA.[30] There is a large hydrophobic cavity present in subdomain IIA that many drugs can also bind. The crystal structure of HSA was taken from the Brookhaven Protein Data Bank (entry codes 1 h9z).[31] The potential of the 3-D structures of HSA was assigned according to the AMBER 4.0 force field with Kollman-all-atom charges. The initial structures of all the molecules were generated by the molecular modeling software SYBYL 6.9.1.[32] The geometries of these compounds were subsequently optimized using the Tripos force field with Gasteiger–Marsili charges. The AUTODOCK 3.05 program[33,34] was used to calculate the interaction modes between the ligands and HSA. The Lamarckian genetic algorithm (LGA) implemented in AUTODOCK was applied to calculate the possible conformations of the ligands that bind to the protein. During the docking process, a maximum of 10 conformers was considered for this compound. The conformer with the lowest binding-free energy was used for further analysis.

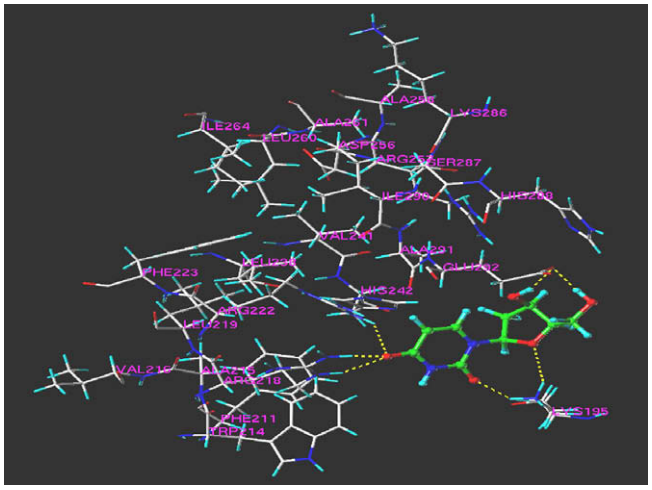

Figure 8. Molecular modeling of interaction between 2′-deoxyuridine and HSA. The residues of HSA and 2′-deoxyuridine are represented using differently colored sticks. The hydrogen bond between the ligands and the protein is indicated by dashed line.

The best energy ranked result is shown in Figure 8. It was obvious that the 2′-deoxyuridine molecule was situated within the subdomain IIA hydrophobic cavity, and 2′-deoxyuridine was adjacent to hydrophobic residues, such as Arg(218), Arg(222), Ala(215), Lys(195), Phe(211), Trp(214), His(242), and Glu(292), of subdomain IIA of HSA. The results of molecular modeling suggest that the interaction between 2′-deoxyuridine and HSA was dominated by hydrophobic forces, which is in agreement with the binding mode proposed from thermodynamic analysis. In addition, there were some hydrogen bonds between 2′-deoxyuridine and residues of HSA such as Lys(195), Arg(218), Arg(222), and Glu(292).

3. Materials and methods

3.1. Materials

Appropriate amounts of HSA (Sigma) were dissolved in doubly distilled water to prepare the stock soln at a final concentration of 2.0×10^{-5} M and this was stored in the dark at 0–4 °C; a 1.0×10^{-3} M 2′-deoxyuridine soln was obtained by dissolving it in doubly distilled water. Tris–HCl buffer soln (0.1 M pH 7.4), 0.5 M NaCl working soln, and 1.0 mg/mL coexistent ions solns were prepared. Unless otherwise mentioned, all chemicals were analytical grade and were used without further purification. Doubly distilled water was used throughout the experiment.

3.2. Apparatus and methods

All fluorescence measurements were carried out on a FP-6500 spectrofluorimeter (JASCO, Japan) and a RF-540 spectrofluorimeter (Shimadzu, Japan) equipped with a thermostat bath and 1.0 cm quartz cells, using 5 nm/5 nm slit widths. A T6 UV–vis spectrophotometer (Purkinje General Instrument Co. Ltd Beijing, China) equipped with 1.0 cm quartz cells was used for scanning the UV spectra. All pH values were measured by a pH-3digital pH-meter (Shanghai Lei Ci Device Works, Shanghai, China) with a combined glass electrode. All calculations were performed on an SGI workstation.

3.3. Fluorescence measurements

Tris–HCl buffer soln (2.0 mL), 2.0 mL NaCl, and appropriate amounts of 2′-deoxyuridine and HSA were added to a 10 mL standard flask and diluted to 10 mL with doubly distilled water. Fluorescence quenching spectra of HSA were obtained at excitation and emission wavelengths of $\lambda_{ex} = 282$ nm and $\lambda_{em} = 300$–450 nm. The synchronous fluorescence spectra were recorded from 280 nm to 340 nm at $\Delta\lambda = 15$ and from 310 to 380 at $\Delta\lambda = 60$ nm.

3.4. Molecular modeling study

The potential of the 3D structures of HSA was assigned according to the AMBER 4.0 force field with Kollman-all-atom charges. The initial structures of all the molecules were generated using the

molecular modeling software SYBYL 6.9.1. The geometries of this drug were subsequently optimized using the Tripos force field with Gasteiger–Marsili charges. The AUTODOCK3.05 program was used to calculate the interaction modes between the drug and HSA. The Lamarckian genetic algorithm (LGA) implemented in AUTODOCK was applied to calculate the possible conformation of the drug that binds to the protein. During the docking process, a maximum of 10 conformers was considered for the drug. The conformer with the lowest binding-free energy was used for further analysis. All calculations were performed on a SGI FUEL workstation.

4. Conclusions

In this paper, the binding reaction between 2′-deoxyuridine and human serum albumin was investigated utilizing fluorescence spectroscopy in combination with molecular modeling. The studies of the interaction of 2′-deoxyuridine and HSA showed that a complex was formed between these species through the static quenching mode. It could be deduced that the binding mode in the binding reaction between 2′-deoxyuridine and HSA was mainly of hydrophobic nature as estimated from the signs of ΔH and ΔS, which was confirmed by the results of molecular modeling. These results may be of significance in pharmacology and clinical medicine.

Acknowledgments

This work was sponsored by the Nature Science Foundation of China (Nos. 20673034, 20772024), the special foundation of Chinese Ministry of Education in 2006, for PhD universities teaching and scientific research (No. 20060476001), and by the Department of Education of Henan Province (No. 2006150012).

References

1. Park, O. J.; Kim, D. Y.; Dordick, J. S. *Biotechnol. Bioeng.* **2000**, *70*, 208–216.
2. Guo, W. X.; Li, X. W.; Tian, G. L.; Ye, Y. H. *Tetrahedron* **2000**, *56*, 3517–3522.
3. Wang, B. J.; Huang, K. *Chinese J. Pharm.* **1987**, *18*, 378–382.
4. Liu, J. Q.; Tian, J. N.; Tian, X.; Hu, Z. D.; Chen, X. G. *Bioorg. Med. Chem.* **2004**, *12*, 469–474.
5. Zilberman, G.; Smith, A. L. *Analyst* **2005**, *130*, 1483–1489.
6. Sawas, A. H.; Pentyala, S. N.; Rebecchi, M. J. *Biochemistry* **2004**, *43*, 12675–12685.
7. Kragh-Hansen, U. *J. Pharmacol. Rev.* **1981**, *33*, 17–53.
8. Xu, C.; Zhang, A. P.; Liu, W. P. *Pestic. Biochem. Phys.* **2007**, *88*, 176–180.
9. Wei, Y. L.; Li, J. O.; Dong, C.; Shuang, S. M.; Liu, D. S.; Huie, C. W. *Talanta* **2006**, *70*, 377–382.
10. Carter, D. C.; Ho, J. X. *Adv. Protein Chem.* **1994**, *45*, 153–203.
11. Sulkowska, A.; Bojko, B.; Równicka, J.; Sulkowski, W. W. *J. Mol. Struct.* **2006**, *792–793*, 249–256.
12. Trynda-Lemiesz, L.; Keppler, B. K.; Koztowski, H. *J. Inorg. Biochem.* **1999**, *73*, 123–128.
13. Miller, J. N. *Proc. Anal. Div. Chem. Soc.* **1979**, *16*, 203.
14. Chang, X. J.; Huang, Y.; He, Q. *Acta Chim. Sinica* **2005**, *63*, 223–228.
15. Chen, G. Z.; Huang, X. Z.; Xu, J. G.; Zheng, Z. Z.; Wang, Z. B. *Methods of Fluorescence Analysis*, 2nd ed.; Science Press: Beijing, 1990.
16. Lakowicz, J. R.; Weber, J. G. *Biochemistry* **1973**, *12*, 4161–4170.
17. Ware, W. R. *J. Phys. Chem.* **1962**, *66*, 455–458.
18. Hu, Y. J.; Liu, Y.; Pi, Z. B.; Qu, S. S. *Bioorg. Med. Chem.* **2005**, *13*, 6609–6614.
19. Leckband, D. A. *Rev. Biophys. Biomol. Struct.* **2000**, *29*, 1–26.
20. Ross, P. D.; Subramanian, S. *Biochemistry* **1981**, *20*, 3096–3102.
21. Neméthy, G.; Cheraga, H. A. *J. Phys. Chem.* **1962**, *66*, 1773–1789.
22. Timasheff, S. N. Thermodynamic of Protein Interactions. In *Proteins of Biological Fluids*; Peeters, H., Ed.; Pergamon Press: Oxford, 1972.
23. Förster, T. In *Modern Quantum Chemistry*; Sinanoglu, O., Ed.; Academic Press: New York, 1996; vol. 3.
24. Yang, P. *The Guide in Bioinorganic Chemistry*; Xi'an Jiaotong Press, 1991.
25. Wu, C. W.; Stryer, L. *Proc. Natl. Acad. Sci. U.S.A.* **1972**, *69*, 1104–1108.
26. Lakowicz, J. R. *Principles of Fluorescence Spectroscopy*; Plenum Press: New York, 1983 [Chapter 10].
27. Cui, F. L.; Fan, J.; Li, J. P.; Hu, Z. D. *Bioorg. Med. Chem.* **2004**, *12*, 151–157.
28. He, W. Y.; Li, Y.; Tian, J. N.; Liu, H. X.; Hu, Z. D.; Chen, X. G. *J. Photochem. Photobiol. A* **2005**, *174*, 53–61.
29. Liang, H.; Huang, J.; Tu, C. Q.; Zhang, M.; Zhou, Y. Q.; Shen, P. W. *J. Ingor. Biochem.* **2001**, *85*, 167–171.
30. Carter, D. C.; He, X. M.; Munson, S. H.; Twigg, P. D.; Gernert, K. M.; Broom, M. B.; Miller, T. Y. *Science* **1989**, *244*, 1195–1198.
31. Petitpas, I.; Bhattacharya, A. A.; Twine, S.; East, M.; Curry, S. *J. Biol. Chem.* **2001**, *276*, 22804–22809.
32. SYBYL Software, Version 6.9.1, St. Louis, Tripos Associates, **2003**.
33. Morris, G. M.; Goodsell, D. S.; Huey, R.; Olson, A. J. *J. Comput. Aided Mol. Des.* **1996**, *10*, 296–304.
34. Morris, G. M.; Goodsell, D. S.; Halliday, R. S.; Huey, R.; Hart, W. E.; Belew, R. K.; Olson, A. J. *J. Comput. Chem.* **1998**, *19*, 1639–1662.